EXTENDED PDF FORMAT
SPONSORED BY

BIO-RAD

http://discover.bio-rad.com



Enhanced Open Ocean Storage of CO2 from Shelf Sea Pumping

Helmuth Thomas, *et al.*

Science **304**, 1005 (2004);
DOI: 10.1126/science.1095491

The following resources related to this article are available online at www.sciencemag.org (this information is current as of January 2, 2007):

Updated information and services, including high-resolution figures, can be found in the online version of this article at:
http://www.sciencemag.org/cgi/content/full/304/5673/1005

A list of selected additional articles on the Science Web sites **related to this article** can be found at:
http://www.sciencemag.org/cgi/content/full/304/5673/1005#related-content

This article has been **cited by** 31 article(s) on the ISI Web of Science.

This article has been **cited by** 2 articles hosted by HighWire Press; see:
http://www.sciencemag.org/cgi/content/full/304/5673/1005#otherarticles

This article appears in the following **subject collections**:
Oceanography
http://www.sciencemag.org/cgi/collection/oceans

Information about obtaining **reprints** of this article or about obtaining **permission to reproduce this article** in whole or in part can be found at:
http://www.sciencemag.org/help/about/permissions.dtl

Downloaded from www.sciencemag.org on January 2, 2007

Science (print ISSN 0036-8075; online ISSN 1095-9203) is published weekly, except the last week in December, by the American Association for the Advancement of Science, 1200 New York Avenue NW, Washington, DC 20005. Copyright c 2006 by the American Association for the Advancement of Science; all rights reserved. The title SCIENCE is a registered trademark of AAAS.

17. R. A. Robie, B. S. Hemingway, *U.S. Geol. Surv. Bull.* **2131**, 462 (1995).
18. See supporting data on *Science* Online.
19. $3FeO_{(s)} + H_2O = Fe_3O_{4(s)} + H_{2aq}$.
20. S. Novak, R. J. Madon, *Ind. Eng. Chem. Fundam.* **23**, 274 (1984).
21. Mass isotopomer distribution of alkanes (C_nH_m) containing zero to n ^{13}C atoms is predicted on the basis of the following multinomial expansion: $M_i = \{n!/[i!(n-i)!]\}(F_{13C})^i(F_{12C})^{n-i}$, where M_i is the mole fraction of the ith mass isotopomer; F_{13C} and F_{12C} are the mole fractions of the ^{13}C and ^{12}C pool, respectively; and i varies from 0 to n.
22. R. C. Brady III, R. Pettit, *J. Am. Chem. Soc.* **102**, 6181 (1980).
23. T. M. McCollom, J. S. Seewald, *Geochim. Cosmochim. Acta* **67**, 3645 (2003).
24. J. S. Seewald, *Geochim. Cosmochim. Acta* **65**, 1641 (2001).
25. R. F. Dias, thesis, Pennsylvania State University (2000).
26. R. F. Dias, K. H. Freeman, M. D. Lewan, S. G. Franks, *Geochim. Cosmochim. Acta* **66**, 2755 (2002).
27. J. S. Seewald, personal communication.
28. B. M. Weckhuysen, I. E. Wachs, R. A. Schoonheydt, *Chem. Rev.* **96**, 3327 (1996).
29. R. L. Burwell Jr., G. L. Haller, K. C. Taylor, J. F. Read, *Adv. Catal.* **20**, 1 (1969).
30. R. Sugisaki, K. Mimura, *Geochim. Cosmochim. Acta* **58**, 2527 (1994).
31. D. S. Kelley *et al.*, *Nature* **412**, 145 (2001).
32. J. J. Brocks, R. Buick, R. E. Summons, G. A. Logan, *Geochim. Cosmochim. Acta* **67**, 4321 (2003).
33. S. Stein, A. Levitsky, O. Fateev, G. Mallard, *The NIST Mass Spectral Search Program for the NIST/EPA/NIH Mass Spectral Library* (National Institute of Standards and Technology, Washington, DC, 1998).
34. We thank M. Berndt, D. Allen, and J. Horita for constructive discussions and R. Knurr for analytical support. Supported by NSF grants 9818908 and 9911471.

Supporting Online Material
www.sciencemag.org/cgi/content/full/1096033/DC1
Materials and Methods
References

26 January 2004; accepted 11 March 2004
Published online 1 April 2004;
10.1126/science.1096033
Include this information when citing this paper.

Enhanced Open Ocean Storage of CO_2 from Shelf Sea Pumping

Helmuth Thomas,* Yann Bozec, Khalid Elkalay, Hein J. W. de Baar

Seasonal field observations show that the North Sea, a Northern European shelf sea, is highly efficient in pumping carbon dioxide from the atmosphere to the North Atlantic Ocean. The bottom topography–controlled stratification separates production and respiration processes in the North Sea, causing a carbon dioxide increase in the subsurface layer that is ultimately exported to the North Atlantic Ocean. Globally extrapolated, the net uptake of carbon dioxide by coastal and marginal seas is about 20% of the world ocean's uptake of anthropogenic carbon dioxide, thus enhancing substantially the open ocean carbon dioxide storage.

Coastal and marginal seas play a key role in the global carbon cycle by linking the terrestrial, oceanic, and atmospheric carbon reservoirs. They host strong biological activity and buffer terrestrial and human impacts before such impacts reach open ocean systems (*1*). The high biological activity, stimulated by both high inputs and efficient use of nutrients, mediates CO_2 drawdown from the atmosphere and subsequent export to the subsurface layer via the biological pump. The ultimate outflow of these CO_2-enriched subsurface waters to the open ocean constitutes the continental shelf pump, a mechanism transferring atmospheric CO_2 into the open ocean, which is thought to substantially contribute to the global ocean's uptake of atmospheric CO_2 (*2*). However, only limited information is available hitherto about these CO_2 fluxes (*3*–*10*). In order to verify this mechanism for the North Sea, we investigated CO_2 uptake by measuring the partial pressure difference of CO_2 (ΔpCO_2) between the North Sea surface waters and the atmosphere. The measurements were carried out during four cruises of 4 weeks each (*11*) as a pilot study in a marginal seas on a consecutive seasonal scale with high spatial resolution.

During the winter situation (Fig. 1A), the surface waters of almost the entire North Sea are in CO_2 equilibrium with the atmosphere. Only the northern eastern part reveals a weak undersaturation, and some areas along the British and southeastern coasts are slightly supersaturated. With the onset of the spring bloom, the entire North Sea becomes strongly undersaturated (Fig. 1B), even in the southern nonstratified region. The remineralization of organic matter exported to the subsurface layer increases the dissolved inorganic carbon (DIC) concentrations in this layer (Fig. 2), whereas the DIC in the surface water decreases. During summer, the ΔpCO_2 distribution (Fig. 1C) shows clear differences between the two biogeochemical provinces of the North Sea: the shallower southern region with a nonstratified water column throughout the year and the deeper, stratified northern region (*12*). The northern region exhibits a strong CO_2 undersaturation up to –150 parts per million (ppm) ΔpCO_2, whereas the south is strongly supersaturated with ΔpCO_2 values up to about 100 ppm. Because of the slowdown of primary production in summer, respiratory processes dominate the carbon cycling in the southern region, generating the observed supersaturation. In the stratified northern region, this respiration further accumulates DIC in the subsurface layer, thereby preventing the increase of the pCO_2 in the surface layer (Fig. 2). The transition in the southern region from strong undersaturation to strong supersaturation from spring to summer points to a decoupling of production and respiratory processes in time and space. This decoupling might allow lateral transport of the organic matter in the southern region (*13*). In fall (Fig. 1D), biological activity decreases, and the mixed layer is deepened in the northern region, allowing the ΔpCO_2 in both regions to begin to equilibrate. In the northern region, the deepening of the mixed layer merges the DIC-enriched, below-thermocline waters (Fig. 2) into the surface layer, and fall storms enhance CO_2 uptake from the atmosphere. In the southern region, decreasing temperatures and continuous CO_2 outgassing diminish the supersaturation.

In order to assess the annual CO_2 air-sea exchange in the North Sea, we assigned ΔpCO_2 data to 13 boxes (Fig. 3C). The data were averaged per season and per box, and the ΔpCO_2 for the remaining months were linearly interpolated. The annual cycles of ΔpCO_2 show that only the most southern region is supersaturated during summer, whereas all other areas remain undersaturated throughout the year, even in winter. The CO_2 air-sea fluxes (Fig. 3B), obtained with the use of 6-hourly wind field data for the time period of observation (*14*), show in correspondence to the ΔpCO_2 features that the North Sea acts as a sink for CO_2 in wide areas throughout the year except for the summer months in the southern region. Highest fluxes are obtained for the spring bloom situation in May, because of the strong undersaturation, but also for October, when the fall storms force the CO_2 uptake, when the CO_2 equilibration of the surface waters has just begun (Fig. 1D). Highest CO_2 release to the atmosphere was obtained for the late summer situation in the southern region because of the strong supersaturation of the surface waters. The annual integration (Fig. 3C) of the CO_2 air-sea fluxes shows that only the most southern region and the adjacent English Channel area act as weak sources for atmo-

Department for Marine Chemistry and Geology, Royal Netherlands Institute for Sea Research, Post Office Box 59, NL-1790 AB Den Burg, Texel, Netherlands.

*To whom correspondence should be addressed. E-mail: hthomas@nioz.nl

Downloaded from www.sciencemag.org on January 2, 2007

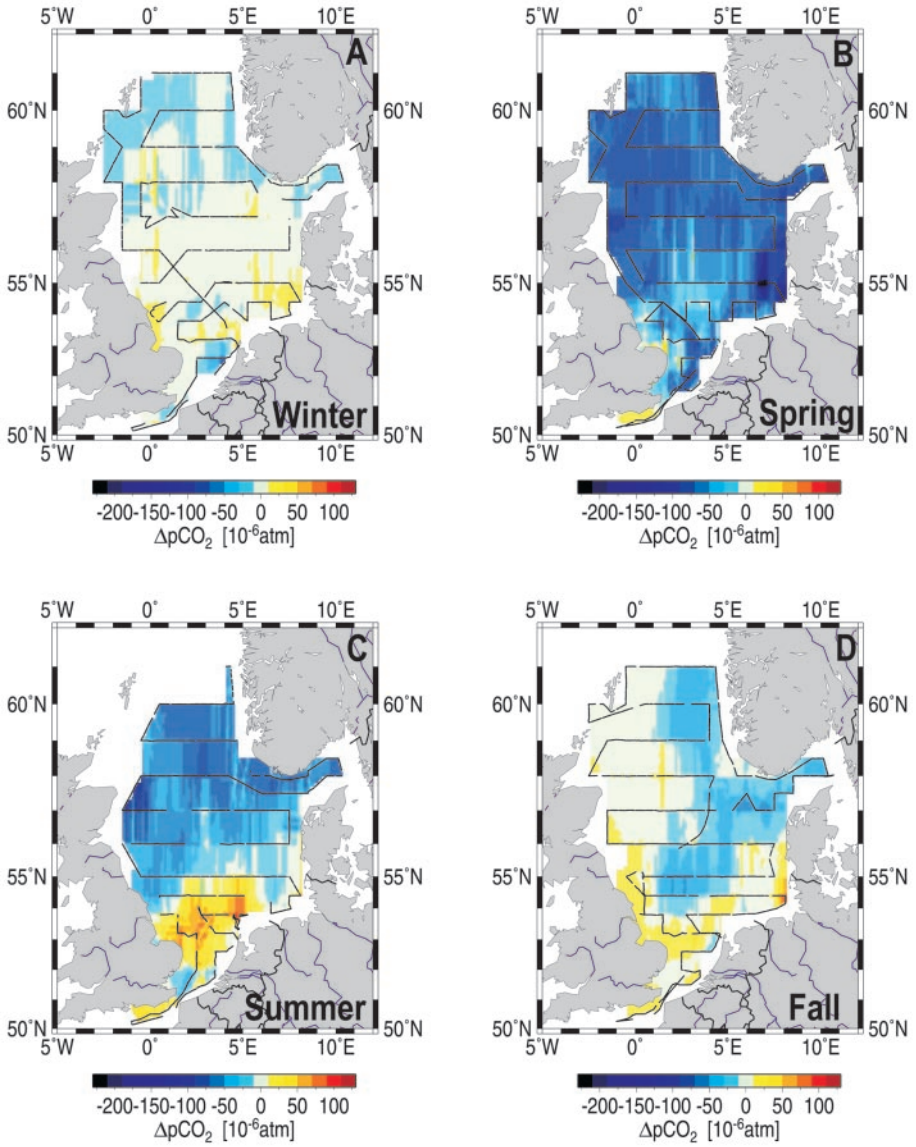


Fig. 1. Distribution of ΔpCO_2 during all four seasons. The surface water data were recorded in 1-min intervals and the atmospheric data in hourly intervals with the use of a continuous measurement system (*23*). Overall, about 90,000 data points were collected. The data are shown relative to the atmospheric pCO_2 observed during each cruise. Negative values denote undersaturation of the surface waters. The cruises (*11*) took place in August to September 2001 (summer), November 2001 (fall), February to March 2002 (winter), and May 2002 (spring) on the Research Vessel *Pelagia*. The same color scale has been applied to all plots.

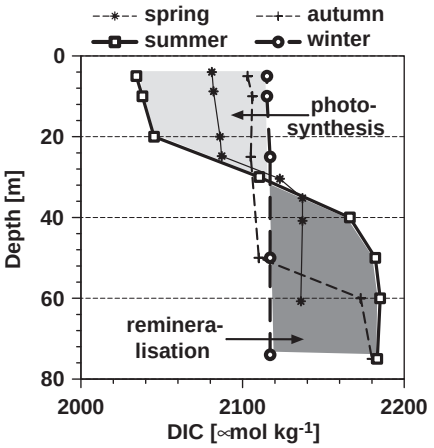


Fig. 2. Seasonal variations of DIC observed at a representative station in the stratified northern North Sea (57°N 2.25°E). The light gray area indicates DIC loss in the surface water between winter and summer because of photosynthetic activity, whereas the darker gray area indicates the DIC increase in the subsurface waters during the same period because of organic matter remineralization [see also (*10*) for comparison].

spheric CO_2, the latter in contrast to earlier findings (*15*). The remaining central and northern parts act as a strong sink roughly north of 54°N. Applying the CO_2 exchange coefficient by Wanninkhof and McGillis (*16*), highest annual uptake rates were obtained for the most northern regions up to 2.5 mol C m^{-2} $year^{-1}$. The basin-wide CO_2 uptake by the North Sea is 1.38 mol C m^{-2} $year^{-1}$ or 8.5×10^{12} g C $year^{-1}$ (excluding the English Channel area). The North Sea thus acts as a rather strong sink for atmospheric CO_2; this conclusion is also in comparison to other regions of the world ocean (*17*).

Less than 1% of the annual primary production, ≈0.13 mol C m^{-2} $year^{-1}$, is ultimately buried in the North Sea sediments (*18*). The largest part of the CO_2, taken up from the atmosphere and processed through the biological food web, is exported to the North Atlantic Ocean. The mechanism of this export (Fig. 4) is evident from the above observations described notably in Fig. 2 and also in Figs. 1 and 3. In the shallower continuously mixed southern area, the carbon metabolism (production and respiration) takes place within the same compartment, thus preventing net CO_2 drawdown. As a consequence, the CO_2 taken up during the spring bloom is released back some time later, causing the CO_2 supersaturation in summer. Over an annual scale, the net CO_2 exchange with the atmosphere is low (Fig. 3). In contrast, the stratification in the northern part allows net CO_2 export from the surface layer to the subsurface layer (Fig. 2). Because this subsurface layer is subjected to major exchange circulation with the North Atlantic Ocean, the CO_2 released in the subsurface waters is largely exported and only partially mixed back into the surface layer during fall and winter convection. The northern North Sea remains undersaturated, and this undersaturation is replenished by atmospheric CO_2, causing the high net CO_2 uptake on an annual scale (Fig. 3). The overall North Sea thus acts as a highly efficient continental shelf pump, exporting ≈93% of the CO_2 taken up from the atmosphere to the North Atlantic Ocean. Considering the North Atlantic Ocean water circulated through the North Sea [55,900 km^3 $year^{-1}$ (*19*)] as the vehicle for this export, we can expect an increase of the DIC concentration within these waters to be on the order of 13 μM.

The DIC and dissolved organic carbon (DOC) exchange fluxes between North Sea and North Atlantic Ocean have been investigated by sampling a section between the Orkney and the Shetland Islands and along 61°N toward Norway. The inflowing branch of North Atlantic Ocean water enters the North Sea along the western side of this section, and the outflow along the Norwegian coast returns the water to the intermediate layers of the North Atlantic Ocean

Downloaded from www.sciencemag.org on January 2, 2007

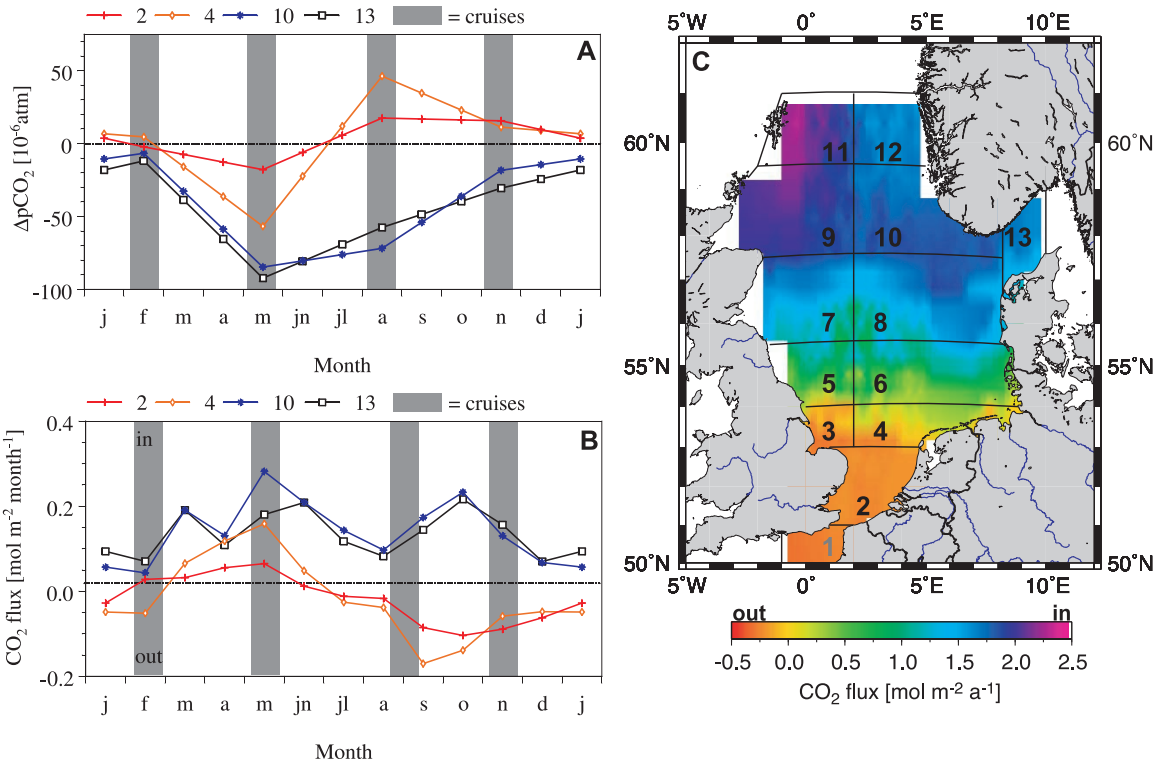


Fig. 3. Annual cycles of the ΔpCO_2 for selected areas in the North Sea (**A**). The shaded areas indicate the time of observations. The fluxes (**B**) have been obtained according to Wanninkhof and McGillis (*16*). (**C**) The annual integration with an average CO_2 uptake of 1.38 mol C m^{-2} $year^{-1}$ for boxes 2 to 13. Alternative parameterizations of the exchange coefficient provide the following fluxes: for (*24*), 0.95 mol C m^{-2} $year^{-1}$; (*25*), 1.68 mol C m^{-2} $year^{-1}$; (*26*), 1.35 mol C m^{-2} $year^{-1}$; and (*27*), 1.28 mol C m^{-2} $year^{-1}$. The average of all five parameterizations is 1.33 mol C m^{-2} $year^{-1}$. There is good agreement among the three more recent parameterizations (*16*, *26*, *27*).

(*12*). A DIC increase of about 24 μM has been observed between the waters entering the North Sea and the waters returning to the North Atlantic Ocean, thus implying a further DIC source to complement the above atmospheric CO_2 input of 13 μM. This DIC is generated by a net loss of DOC in the North Sea as indicated by the higher DOC concentrations found in the inflowing than in the outflowing waters (*19*). The DOC input from the Atlantic Ocean is in part respired to DIC by heterotrophic processes during the water mass transport through the North Sea, generating the additional DIC source of about 11 μM. This DOC loss corresponds to 13% of the overall DOC input to the North Sea. The heterotrophic processes are also evident from the corresponding nutrient budgets (*19*), indicating a net loss of organic nutrients in the North Sea. The heterotrophic processes contribute to the DIC export into the intermediate layers of the North Atlantic Ocean; however, they do not constitute a net carbon flux between the North Sea and the North Atlantic Ocean. Autotrophic processes, which are not evident from the nutrient budgets alone (*19*, *20*), strongly dominate the North Sea carbon cycle, as evident from the CO_2 uptake from the atmosphere, which supplies the net carbon export to the North Atlantic Ocean via the continental shelf pump.

Although coastal and marginal seas cover only 7% of the world ocean's surface (25.2×10^6 km^2) (*1*), their CO_2 uptake from the atmosphere plays a significant role in the global carbon budget. The seasonal amplitudes of the ΔpCO_2 can easily be on the order of 100 ppm, with continuous undersaturation in the North Sea (Fig. 3), or even up to 400 ppm in the Baltic Sea (*6*). In contrast, in the open ocean regimes of similar latitudes, the seasonal amplitudes are only ≈40 ppm (*21*). These much higher ΔpCO_2 cycles cause substantially higher CO_2 uptake from the atmosphere by coastal and marginal seas (*17*), even though, for example, the southern part of the North Sea is a net source for atmospheric CO_2. Extrapolating the CO_2 uptake by the North Sea to the global scale, all coastal seas would have a net CO_2 uptake of 0.4 Pg C $year^{-1}$, which is on the order of 20% of the global ocean's net annual uptake of anthropogenic CO_2 (1.9 ± 0.6 Pg C $year^{-1}$) (*22*). Coastal and marginal seas thus contribute significantly more to the global carbon budget than expected from their surface area alone and enhance the open ocean storage of anthropogenic CO_2.

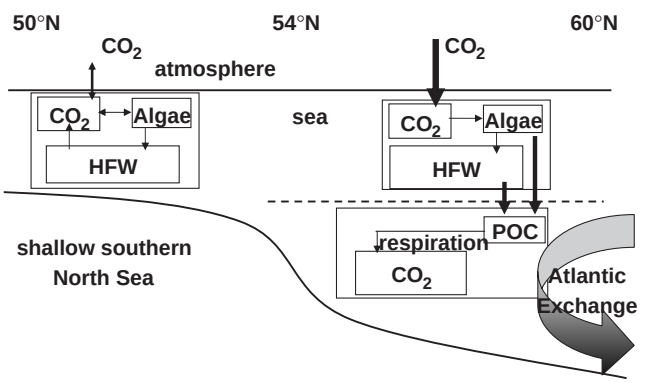


Fig. 4. Sketch of a south-north section through the North Sea. In the shallower southern part production and respiration processes occur in the mixed layer, whereas in the north the respiration processes mainly occur in the separated subsurface layer, which is subjected to the exchange circulation with the North Atlantic Ocean. The broken line indicates the thermocline and the darkening of the arrow implies the increase of DIC in the North Atlantic Ocean water circulated through the North Sea.

References and Notes

1. J.-P. Gattuso, M. Frankignoulle, R. Wollast, *Annu. Rev. Ecol. Syst.* **29**, 405 (1998).
2. S. Tsunogai, S. Watanabe, T. Sato, *Tellus* **51B**, 701 (1999).
3. K.-K. Liu, K. Iseki, S.-Y. Chao, in *The Changing Ocean Carbon Cycle: A Midterm Synthesis of the Joint Global Ocean Flux Study*, R. B. Hanson, H. W. Ducklow, J. G. Field, Eds. (Cambridge University Press, Cambridge, 2000), pp. 187–239.
4. K.-K. Liu *et al.*, *Eos* **81**, 641 (2000).
5. C.-T. A. Chen, K.-K. Liu, R. MacDonald, in *Ocean Biogeochemistry: A Synthesis of the Joint Global Ocean Flux Study (JGOFS)*, M. J. R. Fasham, Ed. (Springer, Berlin, Heidelberg, 2003), pp. 53–97.

Downloaded from www.sciencemag.org on January 2, 2007

6. H. Thomas, B. Schneider, *J. Mar. Syst.* **22**, 53 (1999).
7. C.-T. A. Chen, S.-L. Wang, *J. Geophys. Res.* **104**, 20,675 (1999).
8. S. Kempe, K. Pegler, *Tellus* **43B**, 224 (1991). The authors estimated an uptake of 1.4 mol CO_2 m^{-2} $year^{-1}$ from the atmosphere from pH and alkalinity observations during May and June 1986.
9. C. Osterroht, H. Thomas, *J. Mar. Syst.* **25**, 33 (2000).
10. H. Thomas, V. Ittekkot, C. Osterroht, B. Schneider, *Limnol. Oceanogr.* **44**, 1999 (1999).
11. H. Thomas, "Shipboard report of the RV Pelagia cruises 64PE184, 64PE187, 64PE190 and 64PE195" (Royal Netherlands Institute for Sea Research, Den Burg, Texel, Netherlands, 2002).
12. L. Otto *et al.*, *Neth. J. Sea Res.* **26**, 161 (1990).
13. A. V. Borges, M. Frankignoulle, *J. Mar. Syst.* **19**, 251 (1999).
14. The European Centre for Medium-Range Weather Forecasts is available online at http://www.ecmwf.int/index.html.
15. A. V. Borges, M. Frankignoulle, *J. Geophys. Res.* **108**, 10.1029/2000JC000571 (2003).
16. R. Wanninkhof, W. R. McGillis, *Geophys. Res. Lett.* **26**, 1889 (1999).
17. For convenience, we give the area-specific CO_2 uptake for selected areas. Positive values denote an uptake by the marine area. English Channel (grid box 1 in Fig. 3C), −0.3 mol CO_2 m^{-2} $year^{-1}$ (area covered by this study is 15,840 km^2); southern North Sea (grid boxes 2 to 4), −0.2 mol CO_2 m^{-2} $year^{-1}$ (72,926 km^2); northern North Sea (grid boxes 5 to 13), 1.7 mol CO_2 m^{-2} $year^{-1}$ (438,612 km^2); entire North Sea (grid boxes 2 to 13), 1.38 mol CO_2 m^{-2} $year^{-1}$ (511,540 km^2); Baltic proper, 0.9 mol CO_2 m^{-2} $year^{-1}$ (129,000 km^2) (*6*); East China Sea, 2 mol CO_2 m^{-2} $year^{-1}$ (0.9×10^6 km^2) (*7*); North Atlantic Ocean between 14°N and 50°N, 1.2 mol CO_2 m^{-2} $year^{-1}$ (27.1×10^6 km^2) (*21*); world oceans, 0.5 to 0.6 mol CO_2 m^{-2} $year^{-1}$ (360×10^6 km^2) (*21*, *22*).
18. H. De Haas, T. C. E. Van Weering, H. De Stigter, *Cont. Shelf Res.* **22**, 691 (2002).
19. H. Thomas *et al.*, in *Carbon and Nutrient Fluxes in Global Continental Margins*, L. Atkinson, K.-K. Liu, R. Quinones, L. Talaue-McManus, Eds. (Springer, New York, in press).
20. H. Thomas, J. Pempkowiak, F. Wulff, K. Nagel, *Geophys. Res. Lett.* **30**, 10.1029/2003GL017937 (2003).
21. T. Takahashi *et al.*, *Deep-Sea Res. Part II Top. Stud. Oceangr.* **49**, 1601 (2002).
22. J. L. Sarmiento, N. Gruber, *Phys. Today* **55**, 30 (2002).
23. A. Körtzinger *et al.*, *Mar. Chem.* **52**, 133 (1996).
24. P. S. Liss, L. Merlivat, in *The Role of Air-Sea Exchange in Geochemical Cycling*, P. Buat-Ménard, Ed. (D. Reidel, Dordrecht, Netherlands 1986), pp. 113–127.
25. R. Wanninkhof, *J. Geophys. Res.* **97**, 7373 (1992).
26. P. D. Nightingale, P. S. Liss, P. Schlosser, *Geophys. Res. Lett.* **27**, 2117 (2000).
27. P. D. Nightingale *et al.*, *Global Biogeochem. Cycles* **14**, 373 (2000).

28. The excellent cooperation of the captains, the crews of Research Vessel *Pelagia*, and the scientific staff is gratefully acknowledged. We thank Deutsches Klimarechenzentrum, Deutscher Wetterdienst, and J. Pätsch for making available the European Centre for Medium-Range Weather Forecasts wind data. This study has been encouraged by and contributes to the Land-Ocean Interactions in the Coastal Zone core project of the International Geosphere-Biosphere Program. It was supported by the Research Council for Earth and Life Sciences (ALW) of the Netherlands Organization for Scientific Research (NWO) and the Dutch-German bilateral cooperation Netherlands-Bremen Oceanography. The comments by two anonymous reviewers, V. Ittekkot, and G. Herndl greatly helped improve an earlier version of the manuscript.

9 January 2004; accepted 13 April 2004

Reduction of Particulate Air Pollution Lowers the Risk of Heritable Mutations in Mice

Christopher M. Somers,[1] Brian E. McCarry,[2] Farideh Malek,[3] James S. Quinn[1]*

Urban and industrial air pollution can cause elevated heritable mutation rates in birds and rodents. The relative importance of airborne particulate matter versus gas-phase substances in causing these genetic effects under ambient conditions has been unclear. Here we show that high-efficiency particulate-air (HEPA) filtration of ambient air significantly reduced heritable mutation rates at repetitive DNA loci in laboratory mice housed outdoors near a major highway and two integrated steel mills. These findings implicate exposure to airborne particulate matter as a principal factor contributing to elevated mutation rates in sentinel mice and add to accumulating evidence that air pollution may pose genetic risks to humans and wildlife.

Air pollution has the potential to affect millions of humans worldwide and has been associated with an increased risk of lung cancer (*1*) and of genetic damage in other tissues (*2–5*). To investigate whether air pollution induces heritable DNA mutations, we previously exposed sentinel laboratory mice in situ to ambient air for 10 weeks at two field sites: One was located in an urban-industrial area near two integrated steel mills and a major highway on Hamilton Harbour (Ontario, Canada), and the other was in a rural location 30 km away. Comparison of germline mutation rates at expanded-simple-tandem-repeat (ESTR) DNA loci in mouse pedigrees from each site revealed a 1.5- to 2.0-fold increase in mutation rate at the urban-industrial site, providing evidence that air pollution can cause genetic damage in germ cells, inducing transgenerational effects (*6*). We could not, however, identify causative agents or potential approaches for reducing the mutation risk in urban and industrial areas.

To address these issues, we housed two new groups of sentinel lab mice concurrently for 10 weeks at our earlier urban-industrial site (*6*). The first group was exposed to ambient air, whereas the second group was housed inside a chamber equipped with a high-efficiency particulate-air (HEPA) filtration system. HEPA filtration removes at least 99.97% of particles 0.3 μm in diameter (*7*), and the system we used is rated by the manufacturer to remove up to 99.99% of particles down to 0.1 μm in diameter. In addition, HEPA filtration substantially reduces levels of even smaller ambient particles, down to 0.01 μm (*8*). Mice inside the HEPA filtration chamber were therefore protected from exposure to all airborne particulate matter, with the exception of the smallest ultrafine particles. Simultaneously, we housed third and fourth groups of mice under identical treatment conditions at our rural location, 30 km away, for comparison. Nine weeks after concluding the exposure, we bred the mice and compared germline mutation rates among groups, using pedigree DNA profiling at ESTR loci (*9–12*).

Extensive polymorphism at ESTR loci *Ms6-hm* and *Hm-2* allowed us to determine the parental origin of all mutant bands (tables S1 and S2). The offspring of mice exposed to ambient air at the urban-industrial site inherited ESTR mutations of paternal origin 1.9 to 2.1 times as frequently as the offspring in any of the other three treatment groups (Fig. 1A). Mice exposed to HEPA-filtered air at the urban-industrial site had paternal mutation rates that were 52% lower than those of mice

Table 1. Summary of two-way analysis of variance results for the effect of environmental exposure treatment on per-family, paternal and maternal, single-locus ESTR mutation rates.

Source of variance	*df*	Paternal		Maternal	
		F value	*P* value	*F* value	*P* value
Exposure site	1, 69	7.22	0.0090	3.68	0.0590
HEPA filtration	1, 69	8.03	0.0060	0.07	0.7948
Interaction	1, 69	13.79	0.0004	1.60	0.2098

[1]Department of Biology, [2]Department of Chemistry, McMaster University, 1280 Main Street West, Hamilton, Ontario L8S 4K1, Canada. [3]Lakeland College, School of Environmental Sciences, 5707-47 Avenue West, Vermilion, Alberta T9X 1K5, Canada.

*To whom correspondence should be addressed. E-mail: quinn@mcmaster.ca

Downloaded from www.sciencemag.org on January 2, 2007